Journal of Applied Polymer Science

Mechanical Properties of PLA/PBS Foamed Composites Reinforced by Organophilic Montmorillonite

Jintang Zhou, Zhengjun Yao, Chang Zhou, Dongbo Wei, Shuqin Li
College of Materials and Technology, Nanjing University of Aeronautics and Astronautics, Nanjing 211100, China
Correspondence to: J. Zhou (E-mail: imzjt@126.com)

ABSTRACT: Porous materials have specific properties, such as high surface area, high permeability, lightweight, and low thermal conductivity. In foaming process of thermoplastics, high melt viscosity is indispensable. Neither poly(lactic acid) (PLA) nor poly(butylene succinate) (PBS) has sufficient melt viscosity. In this manuscript, Organophilic montmorillonite (OMMT) was employed to improve the foaming performance PLA/PBS blends. Mechanical tests were undertaken to compare the performance change of PLA/PBS foams before and after reinforcement of OMMT. The compression feature of PLA/PBS foams was discussed. X-ray diffraction (XRD) and scanning electron microscopes were performed to investigate the interaction between OMMT and PLA/PBS foams and the influence of OMMT on cell structure. The results indicated that OMMT can improve the effect of foaming markedly. With 3 wt % OMMT, The compressive strength, flexural strength, and impact strength raised up to 9.2 MPa, 14.0 MPa, and 31.2 kJ/m^2, respectively, and the average size of cells changed from 475.6 to 261.4 μm. FT-IR, TGA, and XRD analysis suggested that CTAC has inserted into the Na-MMT platelets and OMMT platelets are more likely to be intercalated or completely separated in PLA/PBS matrix. © 2014 Wiley Periodicals, Inc. J. Appl. Polym. Sci. **2014**, *131*, 40773.

KEYWORDS: blends; foams; mechanical properties; thermogravimetric analysis (TGA)

Received 19 January 2014; accepted 26 March 2014
DOI: 10.1002/app.40773

INTRODUCTION

In recent years, the extensive use of nonbiodegradable plastics has led to serious environmental pollution because of their nonbiodegradability. Biodegradable polymers are considered to be a suitable, environmentally benign replacement to current petrochemical-based polymers. Recently, interest in these polymers is spurred on by the increasing costs and eventual depletion of petrochemicals feedstocks, concern for the global environment and greenhouse gases, and a general paradigm shift towards sustainable manufacturing.[1–3] Poly(lactic acid) (PLA), which has been widely used in biomedical applications because of its good biocompatibility and various physical properties, is originated from renewable resource-based materials (starch-rich products like wheat, corn, and so on) and grabs much interest in plastics industry today because of its environmental friendly nature. However, its brittleness is a serious defect for many applications. In order to improve its toughness, PLA is often blended with poly(butylene succinate) (PBS). PBS is another biodegradable polymer which has many interesting properties such as excellent toughness and high chemical resistance. Excellent comprehensive mechanical properties will be achieved by blending PLA and PBS.[4–6]

Porous materials have specific properties, such as high surface area, high permeability, lightweight, and low thermal conductivity. Foaming is the simplest and most commonly used production method to prepare polymeric porous materials. In foaming process of thermoplastics, high melt viscosity is critical. Unfortunately, neither PLA nor PBS has sufficient melt viscosity.[7–12] There are several ways to increase the melt viscosity of PLA, such as copolymerization, reaction extrusion, radiation crosslinking and nano-particle blending.[13–20] Nano-particle blending showed rheopexy of shear flow and stress hardening in extensional flow, which leads to high melt viscosity. Thus could be used in the production of high volume expansion ratio foam sheet. Moreover, compared with other methods, blending is much simpler.[21–25]

In this manuscript, Organophilic montmorillonite (OMMT) was employed to improve the foaming performance PLA/PBS blends. Mechanical tests were taken to compare the performance change of PLA/PBS foams before and after reinforcement of OMMT. The compression feature of PLA/PBS foams was discussed. X-ray diffraction (XRD) and scanning electron microscopes (SEM) were performed to investigate the interaction between OMMT and PLA/PBS foams and the influence of OMMT on cell structure.

MATERIALS AND METHODS

Materials

PLA used throughout this experiment was 2002D (ρ=1.24 g/cm^3; Melt flow index = 6 g/10 min), provided by NatureWorks. PBS

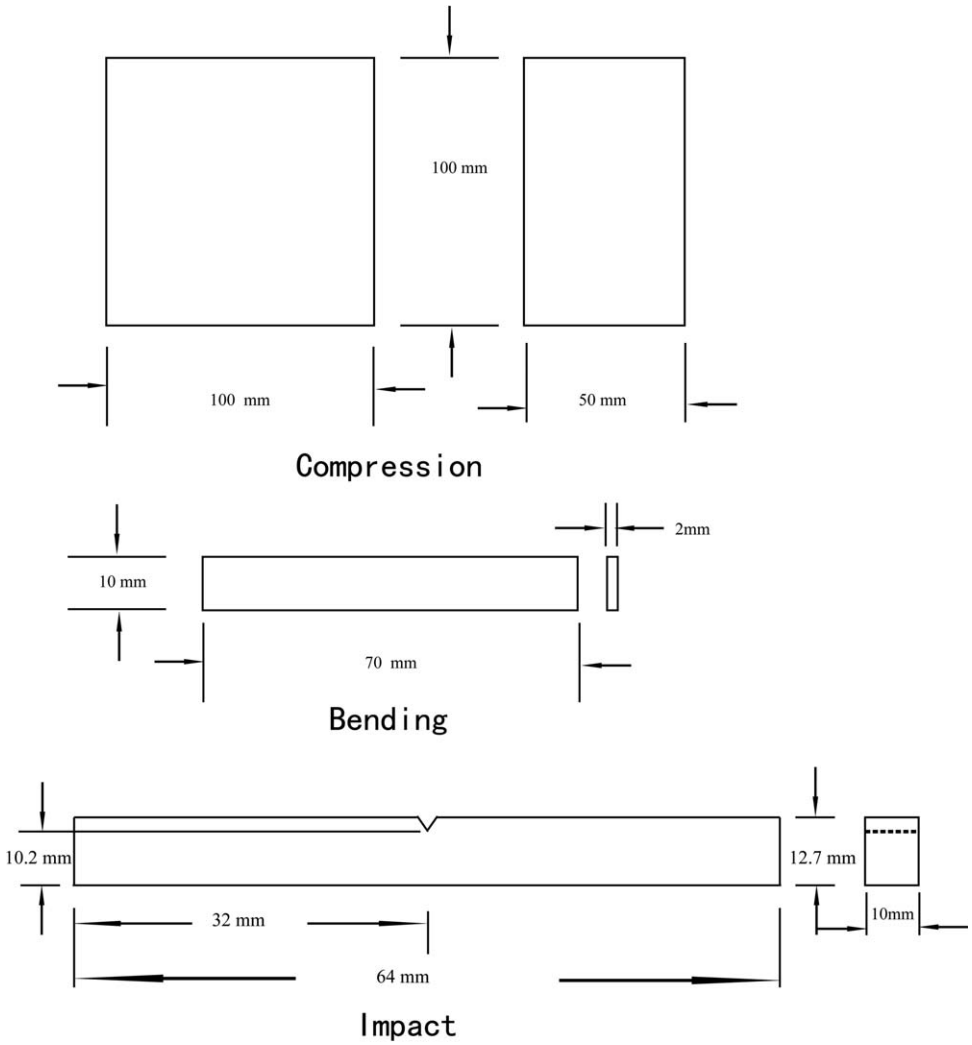

Figure 1. Schematic of mechanical testing samples.

(ρ=1.26 g/cm^3; Melt flow index =10 g/10 min) was supplied by Meilong Group, China. Na-montmorillonite (Na-MMT) was offered by Anqing Hexing Chemical, China. Azodicarbonamide (AC) which was used as blowing agent, ZnO which was used to drop the decomposing temperature of AC, n-Hexadecyltrimethylammonium chloride (CTAC) which was used to prepare organophilic MMT were supplied by Sinopharm Chemical Reagent.

Preparation of OMMT

Five grams of Na-MMT powder was put into a 250 mL beaker, and then 100 mL demonized water was added into it sequentially under stirring in an 80°C water bath. 30 min after that, 6.4 g CTAC was added slowly into the beaker and keep stirring for another 3 hours. Finally, the system was centrifuged and the obtained powder was washed until no Cl^- can be detection. OMMT powder was obtained after drying at 100°C for 72 hours.

Fabrication of PLA/PBS Foams

To obtain PLA/PBS blends, PLA was mixed and granulated with PBS in the proportion of 80 : 20 by a twin-screw granulator (SHJ-30, Nanjing GIANT Machinery, L/D = 30, extrusion rate = 20 kg/h). AC was dispersed with ultrasonic dispersion instrument to remove part of the aggregated grains. ZnO was used to drop the decomposing temperature of AC. To get suitable blowing agent, AC was mixed with ZnO in the proportion of 100 : 20. PLA/PBS blends, OMMT,

Table I. Components of the Samples used in this Manuscript

Samples	PLA/PBS blends (wt %)	OMMT (wt %)	Na-MMT (wt %)	Blowing agent (wt %)
A0	95	0	0	5
A1	94	1	0	5
A2	93	2	0	5
A3	92	3	0	5
A4	91	4	0	5
A5	90	5	0	5
A6	94	0	1	5
A7	93	0	2	5
A8	92	0	3	5
A9	91	0	4	5
A10	90	0	5	5

Table II. Zone Set Temperatures of Twin-Screw Granulator and Injection Molding Machine

Zones	1	2	3	4	5	6
Granulator	120°C	140°C	160°C	170°C	165°C	160°C
Injection machine	120°C	140°C	160°C	170°C	175°C	175°C

and blowing agent were mixed. Then, an injection molding machine (TL-BD4, Haitian Plastics Machinery Group,) was employed in the foam injection molding process. The molds used in the process are ASTM flexural strength specimens. Schematic of the samples was shown in Figure 1. Components of the samples used in this manuscript were listed in Table I and zone set temperatures of both twin-screw granulator and injection molding machine were listed in Table II.

Mechanical Analysis and Micro-Analysis

Compression strength and impact toughness of the samples were tested with a universal testing machine in accordance with ASTM D1621 and ASTM D256, respectively. Samples were immersed in liquid nitrogen for 10 min and broken. The broken surface was vacuum deposited with gold vapor. The internal pore morphology of the broken section was examined by SEM (Hitachi, Japan).

Melt Flow Index

As specified in the ASTM test D1238, melt flow index of the samples were measured with a mass of 2.16 kg at 190°C; the results were expressed in grams per 10 min (six times per sample).

Melt Strength

Melt strength was measured by using Rheotens method with die $L/D = 20/2$ and melt temperature of 185°C. Here, a melt strand was extruded through a capillary die and pulled down within creasing velocity (at constant acceleration 12 mm/s^2) by using a pair of wheels, and the force was measured till the rupture of the melt strand occurred. The average force was defined as melt strength.

Thermal Gravity Analysis

OMMT powders obtained in Preparation of OMMT section and MMT powders were dried and stored under ambient lab conditions (25±1°C and 55±2 %RH) for 72 hours. Then, TG curves of the films were obtained by Shimadzu TGA-50 thermo gravimetric instrument at a flow rate of nitrogen of 40 mL/min. The temperature range is employed from 50°C to 800°C with a ramp rate of 20°C min^{-1}.

FT-IR Spectroscopy

FT-IR spectroscopy is well established as methods of vibrational spectroscopy and has been used for decades as tools for the identification and characterization of groups. FT-IR spectra were measured in the range 4000–500 cm^{-1}.

X-ray Diffraction

Solid film samples were ground using a Wiley mill, and the powder was sieved with a #100 mesh screen. Small-angle X-ray diffraction (SAXD) employed a powder diffractometer (Rigaku MiniFlexII) using Cu-Ka radiation (λ=0.15418 Å). Scattered intensity data were recorded from 2° to 10° (2θ) at a rate of 0.5° per min and a step resolution of 0.02°.

RESULTS AND DISCUSSION

FT-IR Spectroscopy of OMMT

The FT-IR spectrum of Na-MMT and OMMT is shown in Figure 2. In FTIR of Na-MMT, the peak at approximately 1032 cm^{-1} is assigned to horizontal stretching of Si-O bond, and the peak at 3440 cm^{-1} is assigned to -OH stretching vibration of silanol in Na-MMT interlayer. After treatment of CTAC, the characteristic peaks of Na-MMT are also existed in OMMT but the intensity

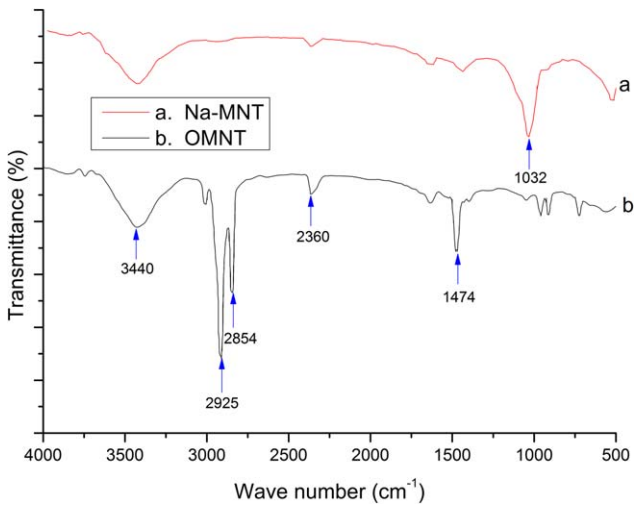

Figure 2. FT-IR spectra for Na-MMT and OMMT. [Color figure can be viewed in the online issue, which is available at wileyonlinelibrary.com.]

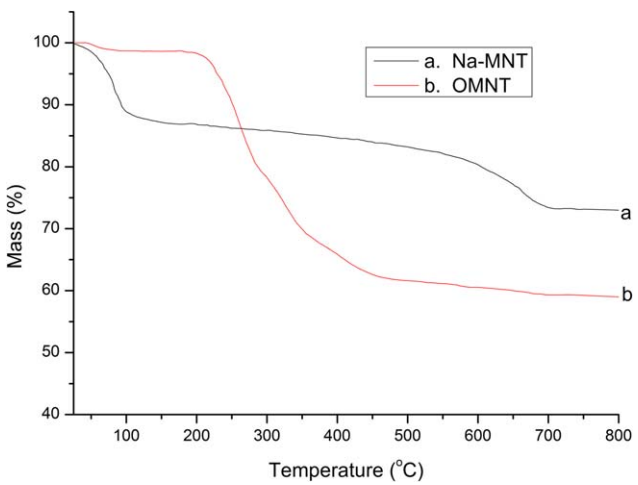

Figure 3. TG curves of Na-MMT and OMMT. [Color figure can be viewed in the online issue, which is available at wileyonlinelibrary.com.]

Table III. Melt Flow Index of PLA/PBS/OMMT Blends

PLA/PBS blends (wt %)	OMMT (wt %)	Melt flow index (g/10 min)	Standard deviation
100	0	6.8	0.24
99	1	6.6	0.25
98	2	5.6	0.36
97	3	5.2	0.38
96	4	5.0	0.78
95	5	4.9	0.82

Table IV. Effect of OMMT on Melt Strength of PLA/PBS Blends

PLA/PBS blends (wt %)	OMMT (wt %)	Melt strength (mN)	Standard deviation
100	0	6.2	0.45
99	1	7.2	0.65
98	2	16.6	0.96
97	3	17.4	0.97
96	4	18.5	1.28
95	5	20.4	1.76

decreased significantly. Furthermore, the appearance of peaks at 2854 and 2925 cm^{-1} are assigned to symmetric stretching and asymmetric stretching of C-H bond in CTAC and the peak at 1474 cm^{-1} is assigned to bending vibration of C-H bond in OMMT interlayer. This indicates that CTAC has inserted into the OMMT layers. The peak at 2360 cm^{-1} corresponds to stretching of CO_2 in the air which is often seen in FT-IR detection.

Thermogravimetric Analysis of OMMT

Interactions between CTAC and Na-MMT could produce changes in thermal behaviors. These changes are expected to be reflected in the differences between TG curves. Figure 3 shows the TG curves of CTAC treated and untreated Na-MMT. The two curves are significantly different from each other. Thermogravimetric analysis (TGA) provides information on the water content of samples. Upon heating, Na-MMT and OMMT undergo several stages of thermal degradation. Up to 150°C, Na-MMT loses about 13% of its weight because of evaporation of moisture on the surface, whereas OMMT loses only about 2% of its weight. This indicates OMMT is hydrophobic and Na-MMT is hydrophilic. Na-MMT manifests a gradual reduction of weight between 150°C and 600°C, which can be contributed to desorption of interlayer water. Further degradation is found on Na-MMT when the temperature continues to creep from 600°C to 700°C, as is evidenced by a faster fall of TG curve. The weight loss after 600°C is considered as the cleavage of the crystal lattice. Unlike Na-MMT, OMMT suffers a fast weight loss and lost much more weight between 200°C and 600°C. Extra weight loss may ascribe the groups imported by CTAC. As CTAC breaks down before 400°C, it is deduced from the diagram that Na-MMT constrains the motion of the groups imported by CTAC and causes the lag of decomposition temperature. In other words, CTAC has inserted into the Na-MMT layers, makes it hard to be affected. It is in accordance with the results of FT-IR spectroscopy. In conclusion, CTAC has inserted into the Na-MMT layers and reduced hydrophile of Na-MMT significantly.

Melt Flow Index and Melt Strength of PLA/PBS Blends Modified via OMMT

Melt flow index is an indirect measure of melt viscosity, with low melt flow rate corresponding to high melt viscosity. Melt flow index of PLA/PBS blends modified via OMMT is represented in Table III. It is evident from Table III that melt flow index declines slowly along with the OMMT concentration, and drops from 6.8 g/10 min to 4.9 g/10 min when OMMT content is 5 wt %. In other words, melt viscosity increases with the growth of OMMT content. Standard deviation is an indication of how much variation or dispersion from the average exists, a high standard deviation indicates that the data points are spread out over a large range of values. Data points of MFR spread out along with the OMMT content. It is not obvious when the amount is less than 3 wt % and there is an abrupt increase when the amount reaches 4 wt %. The increasing of standard deviation may ascribe to the agglomeration of OMMT.

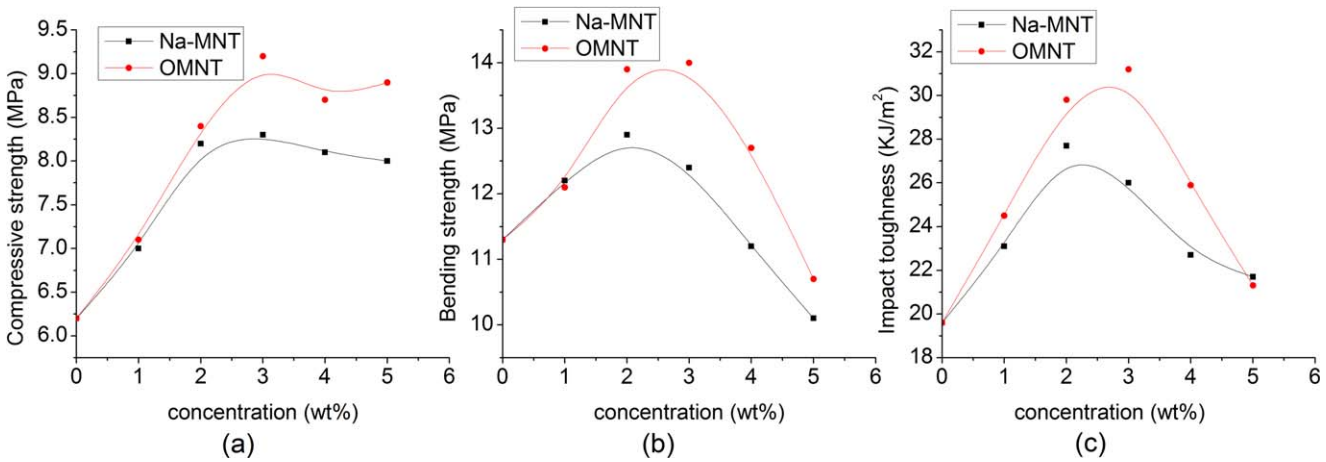

Figure 4. Effects of Na-MMT and OMMT on mechanical properties of PLA/PBS foams. [Color figure can be viewed in the online issue, which is available at wileyonlinelibrary.com.]

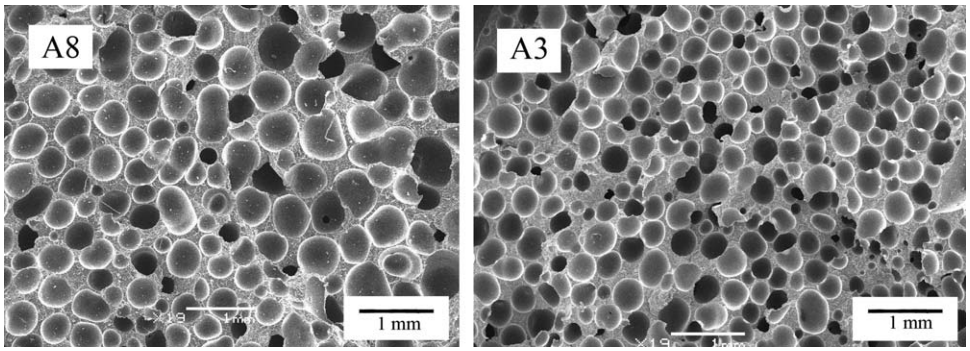

Figure 5. Structure of PLA/PBS foams modified via Na-MMT and OMMT.

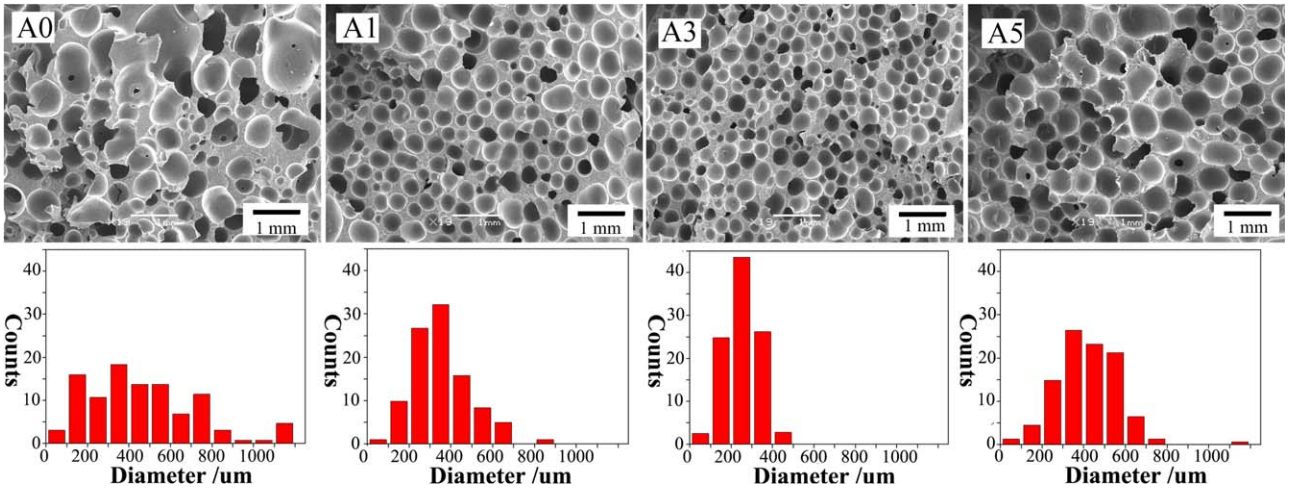

Figure 6. Structure and diameter distributions of PLA/PBS/OMMT foams. [Color figure can be viewed in the online issue, which is available at wileyonlinelibrary.com.]

Melt strength of PLA/PBS blends modified via OMMT is represented in Table IV. It is evident from Table IV that the melt strength of PLA/PBS blends increases along with the OMMT content. Melt strength is increased 168% by using of 2 wt % OMMT and 229% by using 5 wt % OMMT. The result indicates that OMNT can improve melt strength of PLA/PBS blends significantly. It is not obvious when the amount is lower than 1 wt % and there is a sudden enhancement when the amount reaches 2 wt %. Melt strength of blends continues to grow after 2 wt %, but trend seen slowing.

Mechanical Properties of PLA/PBS/OMMT Foams

Compression strength, flexural strength, and impact toughness are three critical factors for studying the mechanical properties of polymeric porous materials. The mechanical properties of PLA/PBS foams reinforced with Na-MMT and OMMT are shown in Figure 4. Compression strength, flexural strength, and impact toughness are increased by addition of both Na-MMT and OMMT. Compression strength is increased 33.9% by using 3 wt % Na-MMT and 48.3% by using 3 wt % OMMT. Na-MMT and OMMT had also an increasing effect on flexural strength; 9.7% by Na-MMT and 23.9% by OMMT. Besides, impact toughness is increased 32.7% by Na-MMT and 59.2% by OMMT. In short, OMMT is much more effective in improving mechanical properties of PLA/PBS foams than Na-MMT. The difference is not obvious when the amount is 1 wt % and there is an abrupt increase when the amount reaches 3 wt %. When

Table V. Cell Size, Cell Density, and Foam Density of PLA/PBS Foams Reinforced by OMMT

Samples	Average diameter (μm)	Square deviation (μm^2)	Cell density (cells·cm^{-3})	Foam density (g·cm^{-3})
A_0	475.6	66,464.2	12,742	0.52
A_1	347.9	17,264.1	32,557	0.48
A_2	260.1	8697.2	77,099	0.41
A_3	261.4	6585.2	76,746	0.42
A_4	330.1	11,335.1	38,099	0.48
A_5	419.4	22,268.8	18,583	0.51

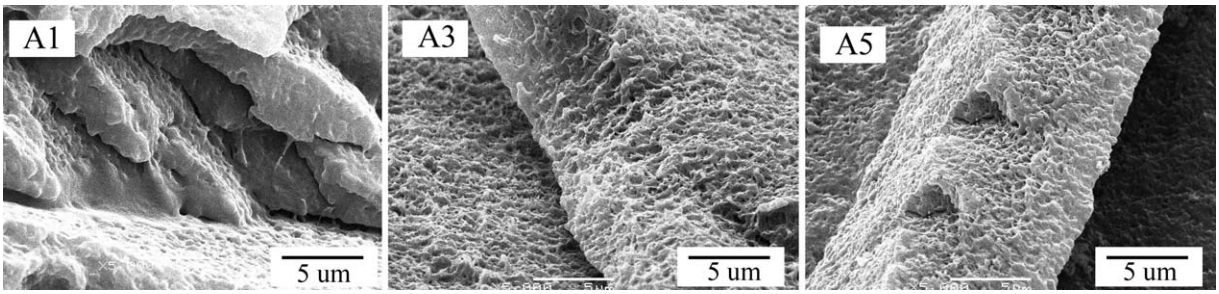

Figure 7. Impact fractograph of PLA/PBS/OMMT foams.

the concentration exceeds 3 wt %, mechanical properties show a downtrend. This may be explained as follows: When the amount of Na-MMT and OMMT is appropriate, platelets of both Na-MMT and OMMT act as physical cross-linking spots and constrain the motion of the molecular chains which result in the enhancement of mechanical properties. OMMT has better compatibility with PLA/PBS foams than Na-MMT. Besides, long-chain fatty amine on OMMT which has been imported by CTAC may entangle with PLA or PBS chain and lead to a better mechanical performance. When the amount is excess, agglomeration happens which lead to the stress concentrations and result in decreasing of the mechanical properties.

Morphology of Foams

Foam morphologies of PLA/PBS modified via Na-MMT and OMMT are illustrated in Figure 5. The content of both Na-MMT and OMMT is 3 wt % which is the optimal dosage for each to get the best mechanical performance. Bubble size of PLA/PBS foams modified via OMMT is smaller and more homogeneous than that via Na-MMT, which indicates uniform foaming. In foam engineering, smaller cell size and uniform foaming augur better mechanical properties. This is consistent with the result of mechanical performance testing.

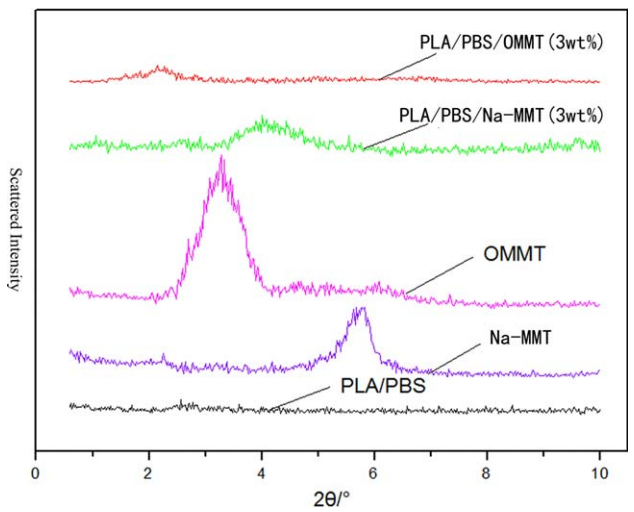

Figure 8. Wide-angle X-ray diffraction patterns for Na-MMT, OMMT, PLA/PBS, PLA/PBS/Na-MMT, and PLA/PBS/OMMT samples. [Color figure can be viewed in the online issue, which is available at wileyonlinelibrary.com.]

The effect of dosage of OMMT on cellular structure was investigated. SEM micrographs presented in Figure 6 provide an overview of the resulting foam morphologies for samples A0, A1, A3, and A5. The data of pore diameters of the foams calculated from the SEM micrographs are also collected and listed in Table V. With the growth of OMMT concentration, bubble size reduced firstly and increased later. As the concentration of OMMT grows from 0 to 3 wt %, the average cell diameter decreases from 475 to 261 μm; Square deviation of cell diameter, which is the indicators of how spread out cell diameter is, decreases from 66464.2 to 6585.2 μm^2; Cell density increases from 12742 to 76746 cells/cm^3; Foam density decreases from 0.52 to 0.42 g/cm^3. As concentration of OMMT continues to accumulate grows from 3 to 5 wt %, a rising tendency of cell diameter is observed. As is well known, the size and morphology of foam are largely determined by the balance between blowing pressures and melt viscosity.[26] As content of blowing agent and foaming process is fixed, blowing pressures of the foams could be considered to be constant. From Melt Flow Index and Melt Strength of PLA/PBS Blends Modified via OMMT section, we already know that melt viscosity and melt strength increases with the growth of OMMT content. This might explain the decline of cell diameter when the content of OMMT is under 3 wt %. On the other hand, OMMT acts as nucleating agents during foaming process. When the concentration exceeds 3 wt %, agglomeration happens and reduces the amount of nucleating agents, which lead to the growth in bubble size.

Figure 7 illustrates impact fractograph of PLA/PBS/OMMT foams. When the dosage of OMMT is 1 wt %, the fracture section is smooth and appears to have a brittleness character. When the dosage of OMMT is 3 wt %, the fracture section is rough and presents ductile fracture features. When the dosage of OMMT increases to 5 wt %, defects which were caused by agglomeration of OMMT are observed. This may be one

Table VI. XRD Character of the Samples Obtained

Samples	2θ (deg)	$d_{(001)}$ (nm)
PLA/PBS	-	-
MMT	5.8	1.52
OMMT	3.3	2.67
PLA/PBS/MMT(3 wt %)	4.1	2.15
PLA/PBS/OMMT(3 wt %)	2.2	4.01

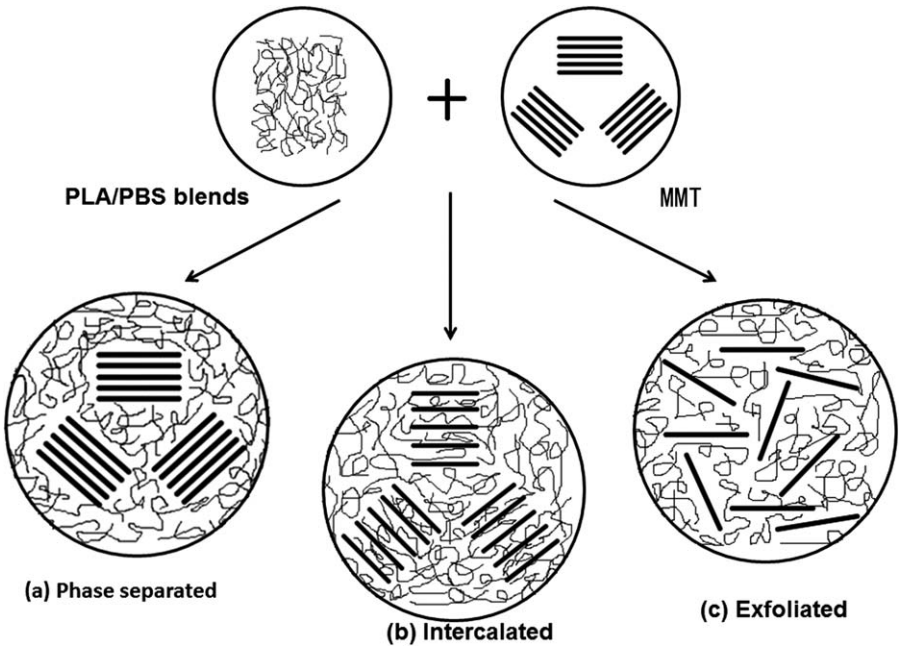

Figure 9. Schematic of the dispersion of MMT in PLA/PBS matrix.

explanation for the decrease in mechanical properties when the content of OMMT is 5 wt %.

XRD Analysis

XRD analysis is a powerful tool for examining the structure of PLA/PBS/OMMT composites. Usually, the peak that indicates the interlayer distance of MMT occurs in the range of 2θ=2–10°. Hence the interlayer distance of MMT can be acquired from the place of diffraction peak in this range. XRD patterns of different samples are shown in figure 8. The distances between interlayer are calculated according to Bragg law and listed in Table VI. XRD patterns for PLA/PBS blends do not have any peaks. XRD patterns for Na-MMT show a peak at 5.8°2θ, whereas OMMT show the corresponding peak at 3.3°2θ. The change in distance is about 1.15 nm, suggests that CTAC has inserted into the Na-MMT platelets. It is in accordance with the results of TGA. The patterns for PLA/PBS/Na-MMT composites clearly show a peak at 4.1°2θ, whereas OMMT show a weak peak near 2.2°2θ. The decline of signal intensity indicates that platelets of OMMT are separated by PLA/PBS blends. Distribution of MMT in PLA/PBS matrix is illustrated in Figure 9. It is possible that MMT platelets may be stacked, intercalated, or divided in the matrix. Na-MMT platelets are likely to be stacked or intercalated, whereas OMMT platelets are more likely to be intercalated or completely separated.

CONCLUSIONS

OMMT was employed to improve the foaming performance PLA/PBS blends. The results indicated that OMMT can improve the effect of foaming markedly. With 3 wt % OMMT, The compressive strength, flexural strength, and impact strength raised up to 9.2 MPa, 14.0 MPa, and 31.2 kJ/m^2 respectively, and the average size of cells changed from 475.6 to 261.4 μm. FT-IR, TGA, and XRD analyses suggested that CTAC has inserted into the Na-MMT platelets and OMMT platelets are more likely to be intercalated or completely separated in PLA/PBS matrix.

ACKNOWLEDGMENTS

This work is supported by the Jiangsu Technology Supporting Project (BE2012169).

REFERENCES

1. Richards, E.; Rizvi, R.; Chow, A.; Naguib, H. *J. Polym. Environ.* **2008**, *16*, 258.
2. Lim, S. K.; Jang, S. G.; Lee, S. I.; Lee, K. H.; Chin, I. J. *Macromol. Res.* **2008**, *16*.
3. Guo, G. P.; Ma, Q. Y.; Zhao, B.; Zhang, D. *Ultrason. Sonochem.* **2013**, *20*, 137.
4. Seo, J.; Lee, K. S. *Polym.-Plast. Technol.*, **2011**, p *51*, 455.
5. Wang, X. X.; Kumar, V.; Li, W. *Cell. Polym.* **2012**, *31*.
6. Kohlhoff, D.; Ohshima, M. *Macromol. Mater. Eng.* **2011**, *296*, 770.
7. Corre, Y. M.; Maazouz, A.; Duchet, J.; Reignier, J. *J. Supercrit. Fluids* **2011**, *58*, 177.
8. Kim, J. U.; Park, B. H.; Lee, M. H. *J. Appl. Polym. Sci.* **2013**, *130*, 2062.
9. Moreira, A. C.; Appoloni, C. R.; Rocha, W.; Oliveira, L. F.; Fernandes, C. P.; Lopes, R. T. *Adv. Appl. Ceramics* **2010**, *109*, 416.
10. Lambert, J.; Graner, F.; Delannay, R.; Cantat, I. *EPL* **2012**, *99*.
11. Annapragada, S. K.; Banerjee, S. *Ind. Eng. Chem. Res.* **2009**, *48*, 3855.
12. Chaudhary, B. I.; Barry, R. P.; Tusim, M. H. *J. Cell Plast.* **2000**, *36*, 397.
13. Li, H.; Deng, H. *J. Appl. Polym. Sci.* **2010**, *118*, 63.

14. Sengwa, R. J.; Choudhary, S. *Bull. Mater. Sci.* **2012**, *35*, 19.
15. Rakhimova, N. A.; Kudashev, S. V. *Russ. J. Gen. Chem.* **2011**, *81*, 369.
16. Liu, X.; Yu, L.; Dean, K.; Toikka, G.; Bateman, S.; Nguyen, T.; Yuan, Q.; Filippou, C. *Int. Polym. Proc.* **2013**, *28*, 64.
17. Liu, L.; Lai, X. *J. Appl. Polym. Sci.* **2010**, *124*, 4107.
18. Chen, X.; Ploehn, H. J. *Carbohydr. Polym.* **2013**, 565.
19. Vacche, S. D.; Plummer, C.; Houphouet-Boigny, C.; Manson, J. *J. Mater. Sci.* **2011**, *46*, 2112.
20. Morales, A. R.; de Paiva, L. B.; Zattarelli, D.; Guimaraes, T. R. *Polimeros-Ciencia E Tecnologia* **2012**, *22*, 54.
21. Keramati, M.; Ghasemi, I.; Karrabi, M.; Azizi, H. *Polym. J.* **2012**, *44*, 433.
22. Li, S.; Li, M. *J. Macromol. Sci., Phys.* **2010**, *49*, 897.
23. Wang, J.; Zhai, W. T.; Ling, J. Q.; Shen, B.; Zheng, W. G.; Park, C. B. *Ind. Eng. Chem. Res.* **2011**, *50*, 13840.
24. Ma, Y.; Liu, Y. *Appl. Math. Mech.-Engl.* **2012**, *33*, 1493.
25. Ma, P. C.; Wang, X. D.; Liu, B. G.; Li, Y.; Chen, S. H.; Zhang, Y. X.; Xu, G. Z. *J. Cell. Plast.* **2012**, *48*, 191.
26. Tai, H. J. *J. Polym. Res.* **2005**, *12*, 457.